Supplementary Materials for

Finger Directed Surface Charges for Local Droplet Motion

Ning Li,[ab] Cunlong Yu,[c] Zhichao Dong*[bc] and Lei Jiang[ab]

[a.] CAS Key Laboratory of Bio-inspired Materials and Interfacial Sciences, Technical Institute of Physics and Chemistry, Chinese Academy of Sciences, Beijing, 100190, P. R. China. Email: dongzhichao@iccas.ac.cn

[b.] School of Future Technology, University of Chinese Academy of Sciences, Beijing, 100049, P. R. China.

[c.] Key Laboratory of Bio-inspired Smart Interfacial Science and Technology of Ministry of Education, School of Chemistry, Beijing Advanced Innovation Center for Biomedical Engineering, Beihang University, Beijing, 100191, P. R. China.

This PDF file includes:

Sections S1

Figs. S1 to S10

Table S1

Captions for Movies S1 to S3

Other Supplementary Materials for this manuscript include the following:

Movies S1 to S3

Section S1. Preparation of substrates with different wettabilities.

Bioinspired Superhydrophobic Surface: The superhydrophobic substrate was prepared by the combination of the deposition and the template coating described as follows.[1,2] The commercial silica plate was cleaned with acetone, ethanol, and purified water and O_2 plasma-treated at 200 W for 10 min before use. The substrate was placed on a carbon source, and the carbon nanoparticle layer was deposited on the silica substrate. Then, the substrate was placed in an airproof petri dish containing 1 ml of aqueous ammonia solution and 1 ml of tetraethoxysilane (TES), and the carbon nanoparticles were gradually coated with the silica shells *via* chemical vapor deposition.[3,4] This process was carried out for 48 hours. Finally, the substrate covered with the silica/carbon nanocomposite was calcinated at 600 °C for 4 hours to remove the carbon nanoparticles, and put together with 0.5 ml of (heptadecafluoro-1, 1, 2, 2-tetradecyl) trimethoxysilane in a vacuum dryer. Finally, the substrate showed superhydrophobicity.

Bioinspired Hydrophobic Surface: A silica plate was cleaned with acetone, ethanol, and deionized water. Then, after treated by O_2 plasma at 150 W for 5 min, it was put in a vacuum dryer together with 0.5 ml of (heptadecafluoro-1, 1, 2, 2-tetradecyl) trimethoxysilane.[5] The vacuum dryer stayed at 80°C for 6 hours, and the plate showed hydrophobicity.

Bioinspired Slippery Surface: The commercial silica plate was cleaned with acetone, ethanol, and purified water and O_2 plasma-treated at 200 W for 10 min. The PDMS covered silica substrate is soaked for in silicone oil 24 hours.[6,7] Then, the substrate was cleaned with water.

Hydrophobic Silica Surface: A silica plate was cleaned with acetone, ethanol, and deionized water. Then, it was processed by O_2 plasma (150 W, 5 min) and put in a vacuum dryer together with 0.5 ml of (heptadecafluoro-1, 1, 2, 2-tetradecyl) trimethoxysilane. The vacuum dryer stayed at 80°C for 6 h, and the plate showed hydrophobicity.

PTFE Hydrophobic Surface: PTFE sheets were sanded with different sizes of sandpaper, and then cleaned with water and ethanol.

Hydrophilic Surface: The clean silica surface showed hydrophilicity. First, the glass substrate was cleaned by boiling in a mixture of 30% H_2O_2 and 98% H_2SO_4, 7:3 v/v for 30 min, and cleaned by acetone and ethanol respectively, rinsed by deionized water several times and blown dry with nitrogen gas.

References

1 Yang, G.; Cao,Y.; Fan, J.; Liu, H.; Zhang, F.; Zhang, P.; Huang, C.; Jiang, L.; Wang, S. Rapid Generation of Cell Gradients by Utilizing Solely Nanotopographic Interactions on a Bio-Inert Glass Surface. *Angew. Chem. Int. Ed.* **2014**, 126, 2959-2962.

2 Yang, G.; Liu, H.; Liu, X.; Zhang, P.; Huang, C.; Xu, T.; Jiang, L.; Wang, S. Underwater-Transparent Nanodendritic Coatings for Directly Monitoring Cancer Cells. *Adv. Healthcare Mater.* **2014**, 3, 332-337.

3 Stober, W.; Fink, A.; Bohn, E. *J.* Controlled growth of monodisperse silica spheres in the micron size range. *Colloid Interface Sci.* **1968**, 26, 62-69.

4 Deng, X.; Mammen, L.; Zhao, Y.; Lellig, P.; Muellen, K.; Li, C.; Butt, H. J.; Vollmer, D. Transparent, thermally stable and mechanically robust superhydrophobic surfaces made from porous silica capsules. *Adv. Mater.* **2011**, 23, 2962-2965.

5 Li, N.; Wu, L.; Yu, C.; Dai, H.; Wang, T.; Dong, Z.; Jiang, L. Ballistic jumping drops on superhydrophobic surfaces via electrostatic manipulation. *Adv. Mater.* **2018**, 30, 1703838.

6 Wong, T. S.; Kang, S. H.; Tang, S. K. Y.; Smythe, E. J.; Hatton, B. D.; Grinthal, A.; Aizenberg, J. Bioinspired self-repairing slippery surfaces with pressure-stable omniphobicity. *Nature* **2011**, 477, 443.

7 Yu, C.; Zhang, L.; Ru, Y.; Li, N.; Li, C.; Gao, C.; Dong, Z.; Jiang, L. Drop Cargo Transfer via Unidirectional Lubricant Spreading on Peristome-Mimetic Surface. *ACS Nano*, **2018**, 12, 11307-11315.

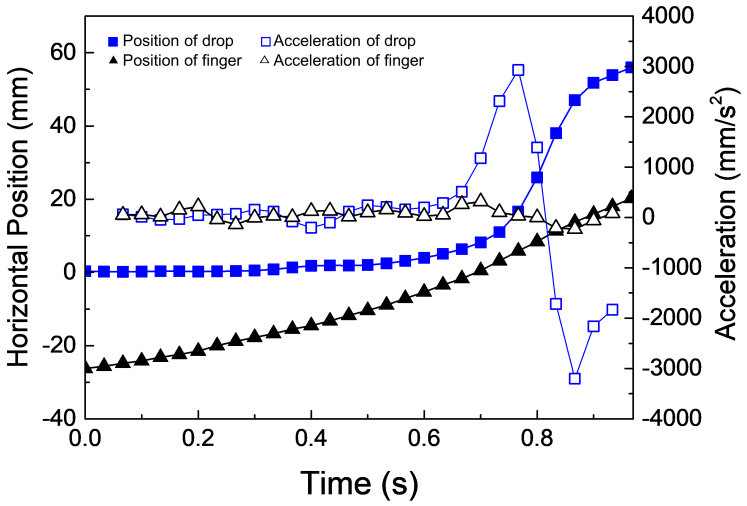

Fig. S1. Plots of acceleration *a* and horizontal positions *x* against time for the drop and finger in Fig. 1. Horizontal position, *x*, as a function of time, *t*. Each curve is fitted by a quadratic function (drawn with a solid line), from which we deduce the acceleration (drawn with a hollow line). The acceleration *a* increases as the distance between the drop and finger decreases. The acceleration increases to 3000 mm s^{-2} and then decreases to -3000 mm s^{-2} in the movement process.

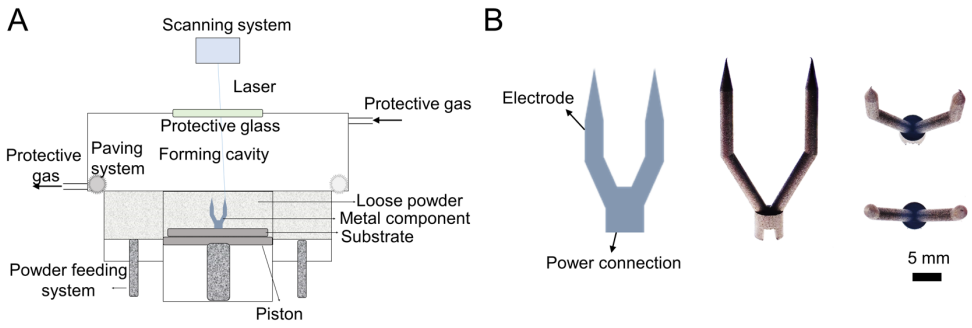

Fig. S2. 3D Metal printing schematic and characterization of the metal electrode. (**A**) The structure scheme of the 3D metal print machine and the scheme of the printing process. (**B**) The double metal electrode is symmetric with two conical electrodes.

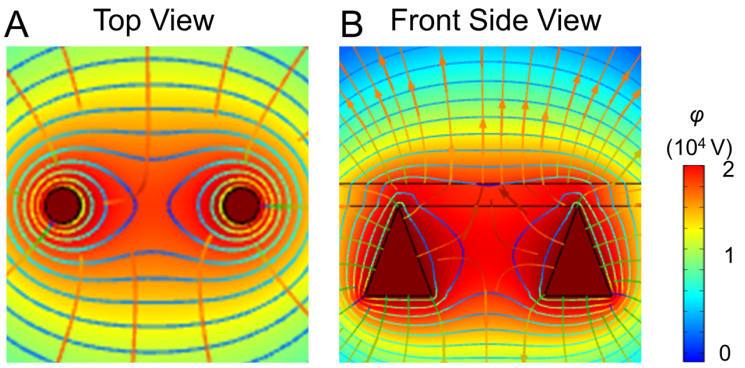

Fig. S3. Theoretical simulation performed by finite-element analysis. The electric field distribution around the insulating substrate is calculated from the top view (**A**) and front side view (B) corresponding to Fig. 2B.

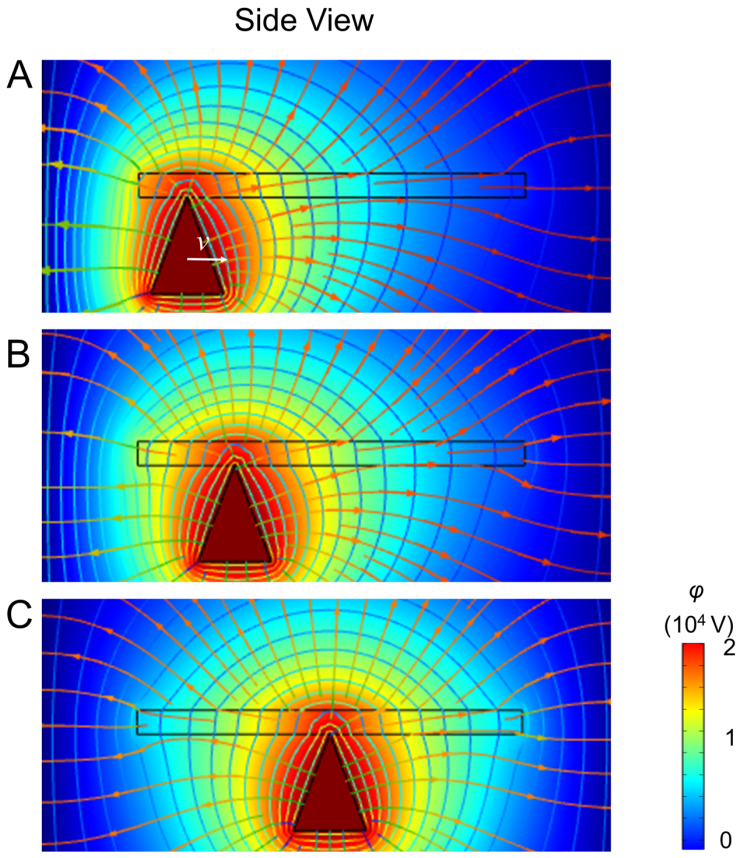

Fig. S4. Distribution of electrostatic fields at different electrode positions performed by a finite-element simulation. The electric field distribution around the insulating substrate when the electrode is in different positions under the substrate.

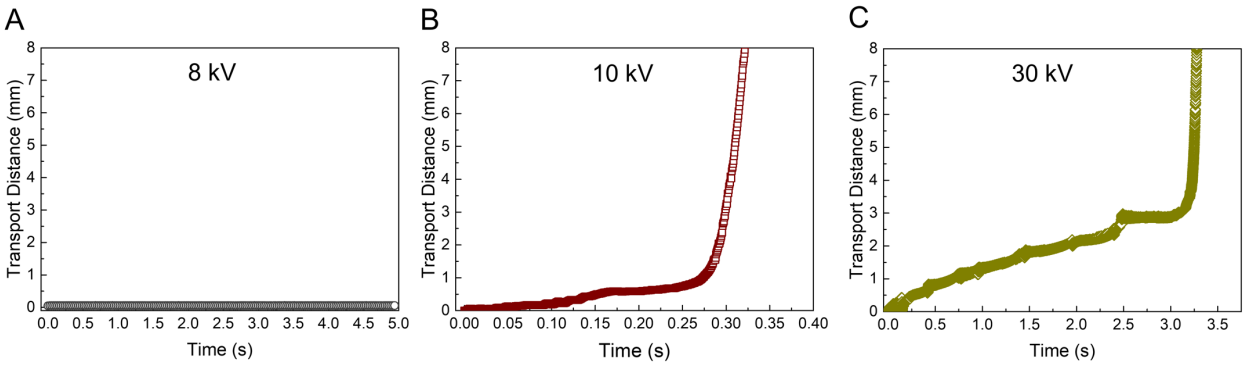

Fig. S5. Plots of horizontal position, *x*, as a function of time, *t*, for droplet local motion on the hydrophobic surface under different voltages. (**A**) The droplet remains at rest after low voltage power turned on. (**B**) At the voltage of 10 kV, the drop first moves slowly, then move with high speed. (**C**) At a higher voltage of 30 kV, the drop moves at a slower speed during most of the transport processes due to the relaxation process, then moves at high speed.

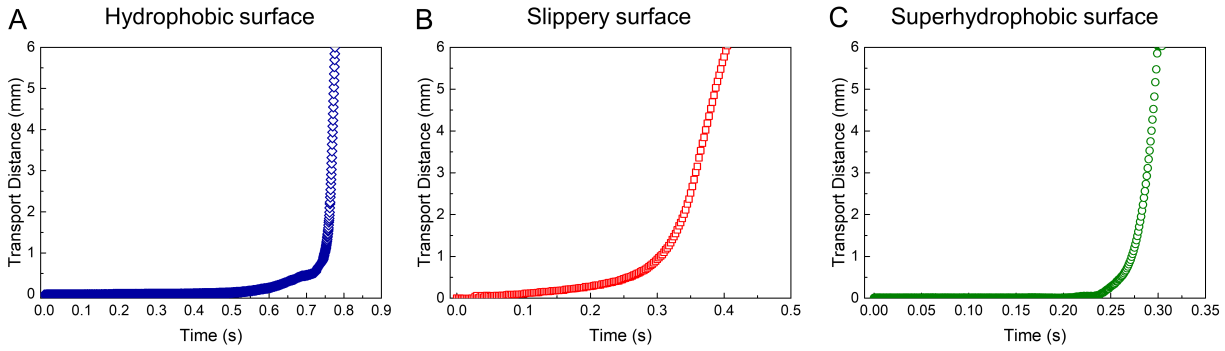

Fig. S6. Comparison of the droplet local motion performances among varied surfaces. Plots of horizontal position, X, as a function of time, t, for droplet local motion on varied surfaces. The motion velocity of the droplet decreases with the surface varied from (A) hydrophobic surface, (B) slippery surface to (C) superhydrophobic surface, corresponding to Fig. 3.

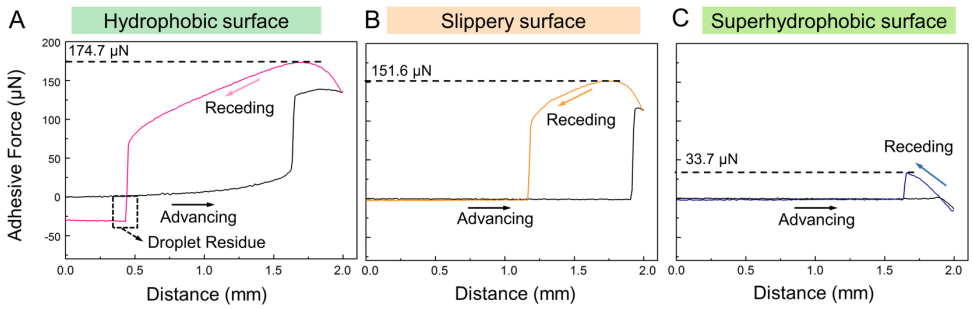

Fig. S7. The relationship between the surface property and the liquid-solid adhesive force for the substrates used in Fig. 3. The adhesive force was measured by contacting a water droplet with a volume of 2 μL on the substrate, then lifting the droplet body and recording the force. The adhesive force between the droplet and the superhydrophobic surface (C) is much lower than that between the droplet and the slippery surface (B) or hydrophobic surface (A).

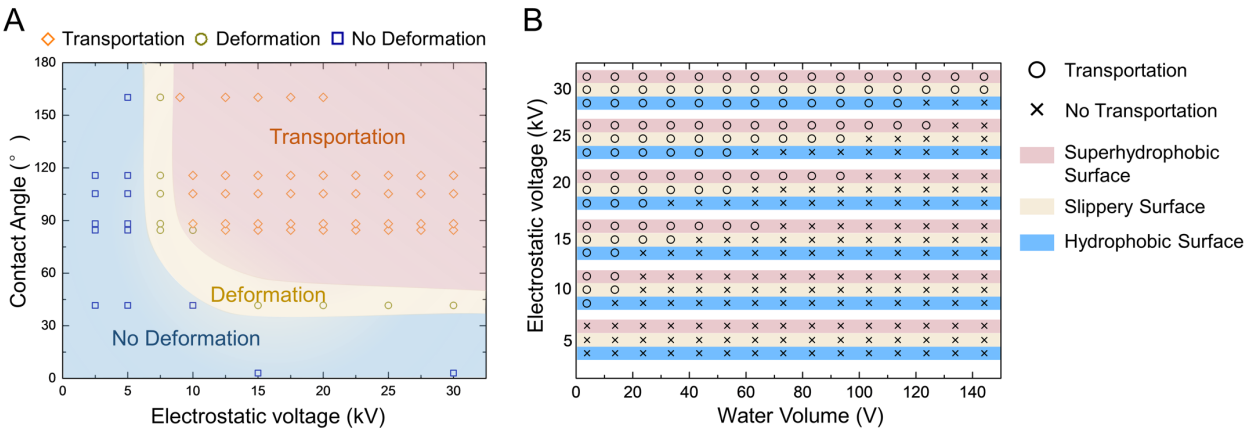

Fig. S8. Phase diagrams associated with electrostatic voltage and droplet local motion on varied surfaces. **(A)** Phase diagrams associated with electrostatic voltage and droplet local motion on varied surfaces. On the hydrophilic surface, the droplet spreads into a film of water, hence the liquid would not deform even increase the electrostatic voltage. Droplets on the hydrophobic surface or the superhydrophobic surface may be deformed when low electrostatic voltage is turned on. When the electrostatic voltage is higher than the threshold of the droplet movement, the droplet can move on the surface. Water droplet is easier to be motivated even in lower voltage on a superhydrophobic surface. **(B)** Generality of droplet local motion with various volumes. Water droplet with 150 μL is possible to be actuated on the superhydrophobic surface.

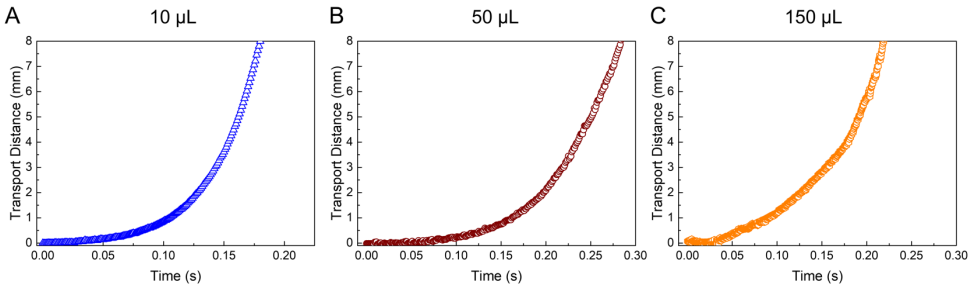

Fig. S9. Droplet local motion with different volumes. Curves of the moving distances against charging time for **(A)** 10 µL droplet under 10 kV, **(B)** 50 µL droplet under 15 kV, and **(C)** 150 µL droplet under 25 kV. The droplet with large volumes can move on the substrate due to the lower adhesion force between the droplet and the surface.

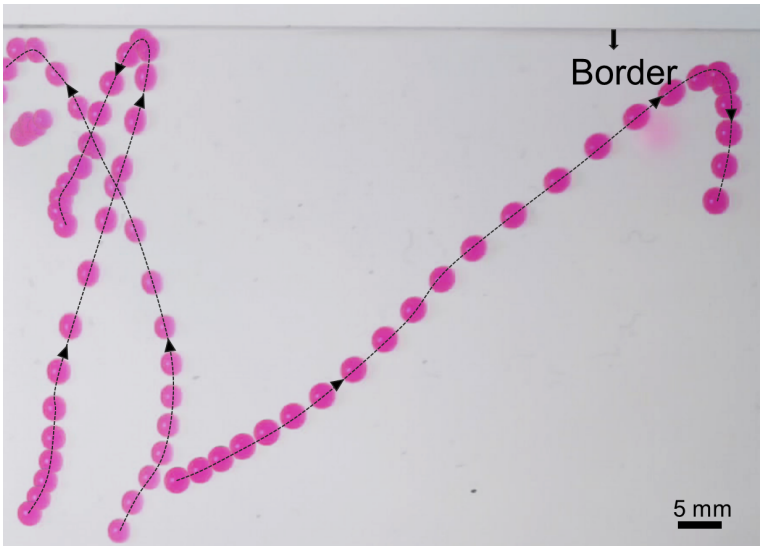

Fig. S10. Self-return of droplet on the superhydrophobic boundary. When close to the border of the substrate, the droplet cannot run out of the border and is repelled by the border to turn around.

Table S1. The mean charges of the droplets moving on substrates with different wettabilities under a varied electrostatic field.

Electrostatic Voltage U (kV)	10	20	30
Hydrophobic surface Q(pC)	73	194	439
Superhydrophobic surface Q(pC)	48	143	395

Movie S1. Finger directed surface charges pattern for droplet local motion.

Movie S2. Droplet local motion on the hydrophobic surface via electrostatic manipulating. Droplet local motion on the surface with varied wettabilities *via* electrostatic manipulating. Local motion of droplet microrobots with varied volumes on the superhydrophobic surface.

Movie S3. Droplet local motion on the surface with varied wettabilities *via* electrostatic manipulating.